THE JOURNAL OF BIOLOGICAL CHEMISTRY VOL. 285, NO. 41, pp. 31253–31260, October 8, 2010

Aquaporin Tetramer Composition Modifies the Function of Tobacco Aquaporins*

Received for publication, February 19, 2010, and in revised form, July 23, 2010 Published, JBC Papers in Press, July 25, 2010, DOI 10.1074/jbc.M110.115881

Beate Otto[‡], Norbert Uehlein[‡], Sven Sdorra[‡], Matthias Fischer[§], Muhammad Ayaz[‡], Xana Belastegui-Macadam[¶], Marlies Heckwolf[‡], Magdalena Lachnit[‡], Nadine Pede[‡], Nadine Priem[‡], André Reinhard[‡], Sven Siegfart[‡], Michael Urban[‡], and Ralf Kaldenhoff[‡1]

From the [‡]Department of Applied Plant Sciences, Institute of Botany, Darmstadt University of Technology, D-64287 Darmstadt, Germany, the [§]Max Planck Institute for Plant Breeding Research, D-50829 Köln, Germany, and [¶]Iden Biotechnology, 31192 Mutilva Baja, Spain

Heterologous expression in yeast cells revealed that NtAQP1, a member of the so-called PIP1 aquaporin subfamily, did not display increased water transport activity in comparison with controls. Instead, an increased CO_2-triggered intracellular acidification was observed. NtPIP2;1, which belongs to the PIP2 subfamily of plant aquaporins, behaved as a true aquaporin but lacked a CO_2-related function. Results from split YFP experiments, protein chromatography, and gel electrophoresis indicated that the proteins form heterotetramers when coexpressed in yeast. Tetramer composition had effects on transport activity as demonstrated by analysis of artificial heterotetramers with a defined proportion of NtAQP1 to NtPIP2;1. A single NtPIP2;1 aquaporin in a tetramer was sufficient to significantly increase the water permeability of the respective yeast cells. With regard to CO_2-triggered intracellular acidification, a cooperative effect was observed, where maximum rates were measured when the tetramer consisted of NtAQP1 aquaporins only. The results confirm the model of an aquaporin monomer as a functional unit for water transport and suggest that, for CO_2-related transport processes, a structure built up by the tetramer is the basis of this function.

Water moves across biological membranes by diffusion. In most living organisms, the rate of water diffusion can be increased via pore-forming transmembrane proteins, the so-called aquaporins. These consist of six-membrane-spanning helices; N and C termini of the proteins face the cytosol. The helix-connecting loops B and E are themselves short helices that dip into the membrane from opposite sides and form the water-conducting channel (1, 2). Aquaporin monomers can assemble into tetramers (3, 4). Evidence for their function as water transport facilitators was observed by results from experiments using heterologous expression systems, such as *Xenopus laevis* oocytes (5). Despite this initially detected function, a facilitated membrane transport for glycerol or volatile substances like CO_2 or NH_3 was postulated (6–9). Plant aquaporins were subdivided into protein groups according to the cellular location in which they have been initially detected and on the basis of sequence similarities (10). Accordingly, the PIPs (plasma membrane-intrinsic proteins) were split into two major groups, the PIP1 and PIP2 aquaporins. Compared with PIP1 proteins, PIP2 proteins have a shorter N-terminal extension and a longer C terminus (11–14). In general, plant PIP2 proteins have been shown to facilitate membrane water transport in heterologous expression systems; however, PIP1 proteins display low or no activity in this respect (8, 11, 15–18). For the human AQP1 as well as for the tobacco PIP1 aquaporin NtAQP1, an increased cellular acidification rate under CO_2-enriched buffer was obtained in oocytes expressing the respective aquaporin in addition to a carbonic anhydrase (9, 19, 20). The observations on NtAQP1, together with the fact that plants deficient in NtAQP1 expression have an increased resistance for CO_2 transport in leaves, lead to the suggestion that some PIP1 aquaporins could conduct CO_2 instead of water, and thus, the term cooporin was created (21–23). Because in plants, PIP1 and PIP2 aquaporins are often expressed in the same tissue, and, as mentioned above, aquaporins tend to form tetramers, it was hypothesized that the formation of aquaporin multimers could have consequences on their membrane water transport activity. In fact, in oocytes, it was shown that membrane integration was more effective when PIP1 and PIP2 were coexpressed (24). Consequently, the measured water transport rates were increased. In maize root protoplasts, it could be demonstrated that fluorescence protein-tagged PIP1 and PIP2 aquaporins were located in close vicinity in the plasma membrane (25, 26). It is, however, not precisely clear whether the proteins in fact form heterotetramers or whether homo-PIP1 and homo-PIP2 tetramers come so close together that the FRET effect could be observed. A consequence for aquaporin specificity has not yet been investigated.

Because the experimental data for NtAQP1 from oocytes imply a function as cooporin and the protein was found to be located in leaf membranes such as the PIP2 aquaporin NtPIP2;1, we were interested in characterizing the effect of NtAQP1 and NtPIP2;1 coexpression on water and CO_2 transport. Oocytes serve as the heterologous expression system for aquaporins even though they show variability between individual cells. Because of technical restrictions, large numbers of repetitions can only be achieved by extraordinary technical efforts over a long period of time. Consequently, studies were performed in yeasts expressing the respective protein encoded by a plasmid-located gene. Because the results rely on clones and large amounts of cell material were readily available, data variation could be minimized.

* This work was supported by a Deutsche Forschungsgemeinschaft grant (to R. K.).

[1] To whom correspondence should be addressed: Applied Plant Sciences, Darmstadt University of Technology, D-64287 Darmstadt, Germany. E-mail: kaldenhoff@bio.tu-darmstadt.de.

At some point during our studies, the results strongly suggested that the proteins not only come close together but form heterotetramers. This leads us to a closer characterization of the effect of the PIP1/PIP2 ratio in a tetramer on water transport or CO_2 transport function.

EXPERIMENTAL PROCEDURES

Cloning and Expression in Yeast—cDNAs encoding tobacco NtAQP1 (accession no. AJ001416) and NtPIP2;1 (accession no. AF440272) were inserted into the pYES-DEST52 yeast expression vector using Gateway™ technology (Invitrogen). For synthesis of artificial tetramers, the complete translated region was amplified using primers with suitable additional restriction sites. The combinations of NtAQP1 and NtPIP2;1 were constructed by restriction/ligation cloning into the pYes2/CT yeast expression vector. Special attention was paid to maintaining the correct reading frame. Fusions of NtAQP1 or NtPIP2;1 and N- or C-terminal halves of YFP (accession no. DQ168994) separated by sequences coding for an eight-amino acid linker (GSGGSGGS) were constructed by recombinant PCR and inserted into the pYes2/CT yeast expression vector pGREG505_2μ and YEplac112_gal by restriction/ligation cloning. The cDNA encoding *Nicotiana tabacum* carbonic anhydrase (accession no. M94135) was inserted into pGREG505 by Drag&Drop cloning (33). To assure a high expression level of carbonic anhydrase, the low copy vector pGREG505 (Euroscarf) was converted into a high copy vector by replacing the low copy origin ARSH/CEN by the 2μ origin of pYES-DEST52 (Invitrogen). All constructs were verified by sequencing. *Saccharomyces cerevisiae* cells of the strain SY1 (34) were transfected by biolistic bombardment as described elsewhere (35). Carbonic anhydrase activity was determined using a mass spectrometer as described by Endeward *et al.* (27). For water permeability measurements, selection of single transformants containing the aquaporin constructs in pYes-DEST52 or pYes2/CT was based on ura3 complementation. Double transformants for CO_2 permeability measurements containing the carbonic anhydrase in addition to the aquaporin constructs were selected by ura3 and leu2 complementation. Yeast transformants were cultured in glucose containing synthetic complete medium without Ura/Leu for 12 h. Cultures were diluted to $A_{600} = 0.6$, and heterologous protein expression was induced for 16 h by changing the medium carbon source from glucose to galactose. For aquaporin-YC/YN fusions (C- or N-terminal half of YFP are designated as YN or YC, respectively), an induction time of 28 h (NtAQP1-YC+NtAQP1-YN, NtAQP1-YC+NtPIP2;1-YN) and 32 h (NtPIP2;1-YC+NtPIP2;1-YN) resulted in a maximum of aquaporin protein abundance. Expression of aquaporin constructs was verified by Western blot analysis. Yeast membrane proteins were separated on SDS-PAGE and electrotransferred onto nitrocellulose membranes. Specific aquaporin content was verified by incubation of nitrocellulose membranes with a NtPIP2;1 or NtAQP1-specific antibody and detection by the Western-Star™ system (Applied Biosystems, Foster City, CA). Yeast strains were *S. cerevisiae* SY1 (Matα, ura3-52, leu2-3112, his4-619, sec6-4^{ts}, GAL2) and W303 (MAT**a**/MATα ADE2/ade2 CAN1/can1-100 CYH2/cyh2 his3-11,15/his3-11,15 LEU1/leu1-c LEU2/leu2-3112 trp1-1:URA3:trp1-3′Δ/trp1-1 ura3-1/ura3-1).

Water Permeability Measurements—Water permeability of intact yeast protoplasts was measured by stopped flow spectrophotometry as described elsewhere (28). The protoplasts were exposed to a 300 mosmol outwardly directed osmotic gradient to induce protoplast swelling. Volume change was followed by the decrease of scattered light intensity in a stopped flow spectrophotometer (SFM-300, Bio-Logic SAS, Claix, France). Quantification of water conductivity was achieved by fitting a single exponential function on the initial 100 ms on the swelling kinetics using the Biokine (Bio-Logic SAS) software. The osmotic water permeability coefficients (P_f) were calculated as described by van Heeswijk and van Os (29) using the rate constant of the exponential decay, the molar volume of water, the external osmolarity after the mixing event, and the initial mean protoplast volume and surface. The initial size of protoplasts was determined by light microscopy. For controls, yeasts expressing the three N-terminal helices of NtPIP2;1 were used throughout. Calculation of P_f values were residing on at least five independent experiments of three independently transformed clones with an average of 20 measurements each ($n \geq 100$).

CO_2-triggered Intracellular Acidification—CO_2-triggered intracellular acidification was measured in yeast cells loaded with fluorescein bisacetate as described previously (28). Cells were suspended in 75 mM NaCl, 25 mM Hepes-NaOH, pH 6. The cell suspension was mixed rapidly (SFM-300, Bio-Logic SAS) in a buffer solution containing 75 mM $NaHCO_3$, 25 mM Hepes-NaOH, pH 6. Uptake of CO_2 resulted in an intracellular acidification and consequently a decrease of fluorescein fluorescence. The exponential time constant of the acidification was determined over the initial 30 ms. CO_2 permeability was calculated as described elsewhere (30). The cell diameter was 5 μm (SY1) and 3.5 μm (W303), giving a surface to volume ratio (S/V) of 1.2×10^4 cm^{-1} (SY1) and 1.7×10^4 cm^{-1} (W303), respectively. The cell size was determined by light microscopy. Yeasts coexpressing carbonic anhydrase and an aquaporin display similar carbonic anhydrase activity. For controls, yeasts expressing the three N-terminal helices of NtPIP2;1 and carbonic anhydrase were used throughout. It was found that these and cells coexpressing other plasma membrane-located proteins (potassium channel, MDL1p) showed almost identical low CO_2-triggered intracellular acidification rates. Calculation of P_{CO2} values were residing on at least 10 independent experiments of three independently transformed clones with an average of 20 measurements each, in a double-blind experimental design ($n \geq 200$).

Bimolecular Fluorescence Complementation—For bimolecular fluorescence complementation emission spectra from yeast expressing NtAQP1-YC+NtAQP1-YN, NtAQP1-YC+NtPIP2;1-YN, NtAQP1-YN+NtPIP2;1-YC, and NtPIP2;1-YC+NtPIP2;1-YN were recorded to confirm YFP-originated fluorescence. Fluorescence was detected from 500 to 750 nm with an excitation filter at 488 nm (PerkinElmer LS 50 B). The measured spectra were matching those published for YFP (31). Specificity of the signals for protein-protein interaction was tested by a fusion protein of YN to Multidrug Resistance Like Protein

(MDL1p), a yeast ABC transporter that was coexpressed with NtAQP1-YC in yeast. No fluorescence over a time period of 34 h was detected.

Colocalization Analysis—Colocalization analysis was done by microscopic observation of fluorescence in the cells using a Leica DM IRB/E. Colocalization analysis was carried out according to Kirber *et al.* (32). FM4-64 staining of cell plasma membranes was achieved by incubation of intact yeast cells for 20–30 min in 15 μM FM4-64 at 4 °C with gentle agitation. For every pair of images (FM4-64 fluorescence image and YFP fluorescence image), a figure of colocalized pixels with a brightness greater than 0 and the background set to 0 was generated. The image was treated with a noise filter according to Ref. 33 to discriminate between signal and noise. Subsequently, all remaining bright pixels were set to 1. From this, a 0–1 matrix was gained, and the original YFP image was multiplied by the 0–1 covariance matrix. The resulting image depicted only pixels from YFP/FM4-64 colocalized signals. Quantification of total fluorescence in the plasma membrane was accessed by comparing the brightness of colocalization image and original YFP fluorescence corrected by the averaged brightness of the respective background. Based on these data, the amount of YFP fluorescence in the plasma membrane could be determined.

Tetramer Composition—Tetramer composition was assessed in plasma membrane preparations from yeast strains expressing NtAQP1-YC in pYes2/CT in SY1, NtPIP2.1 in pYES-DEST52 in SY1, or NtAQP1-YC/NtPIP2.1 (NtPIP2.1 pYES-DEST52 transformed into NtAQP1-YC pGREG505 containing strain SY1). Yeasts were cultivated overnight in a medium depleted from selecting amino acids (−Uracil, −Leucine, or −Ura/−Leu, respectively) with glucose (2% w/v) as a carbon source and then diluted to an $A_{600} = 0.6$. Expression of aquaporins was induced in galactose-containing medium (2% w/v). Isolation of plasma membranes from yeast cells was performed according to Panaretou and Piper (34). 6 g of cells were washed in buffer A (2 mM EDTA, 25 mM imidazole/HCl, pH 7, 0.4 M sucrose) supplemented with protease inhibitors (4 μg/ml pepstatin, 1 mM PMSF, 50 μg/ml leupeptin). 2 Volumes of glass beads (0.5 mm) were added to the cell pellet followed by buffer A just sufficient enough to cover the pellet. After 5 min of vortexing, the mixture was diluted 3-fold with buffer A and centrifuged for 20 min at 530 × *g*. The membranes were collected by a 30-min centrifugation at 22,000 × *g*. The pellet was resuspended in buffer A, loaded on a sucrose-step gradient (1.1, 1.65, and 2.25 M sucrose in 2 mM EDTA, 25 mM imidazole/HCl, pH 7; 9-ml each) and centrifuged for 15 h at 80,000 × *g*. Membranes were obtained from the 2.25/1.65 M interface. The combined plasma membrane fractions were washed with 20 mM Tris/HCl, pH 7.5, 150 mM NaCl, 10% glycerol. Solubilization of aquaporins was tested with 16 different detergents. Yield and purity of aquaporins was assessed by Western blot with a specific antibody. Dodecylmaltoside (DDM)[2] was identified as a suitable detergent. The aggregation state of DDM-treated aquaporins was analyzed by analytical size exclusion chromatography on Superdex 200 PC 3.2/30 following the manufacturer's protocol (Amersham Biosciences). Under these conditions, the tetrameric state with a molecular mass of at least 120 kDa was favored.

Solubilization of Aquaporins—Solubilization of aquaporins was achieved in the following solution: 10 mg/ml membranes, 10% glycerol, 2 mM β-mercaptoethanol, and 2% DDM (*n*-dodecyl-β-maltoside, Glycon). The solution was incubated for 2 h at 4 °C with gentle shaking; followed by a 15-min centrifugation at 130,000 × *g*. The supernatant was applied to a NAP-5 column (GE Healthcare) to change the DDM concentration to 0.05%. Aquaporin tetramers were separated from monomers and sorted by size using gel filtration column chromatography (GE Healthcare C10/40 packed with Superdex 200 prep grade) connected to an Äktaprime (GE Healthcare) at a flow rate of 0.5 ml/min. The eluent was collected in 0.5-ml aliquots. Running buffer was 20 mM Tris/HCl, pH 7.5, 150 mM NaCl, 10% glycerol, 0.05% DDM. All fractions corresponding to a molecular mass larger than 80 kDa were diluted with 1 volume of denaturing buffer (8 M urea, 100 mM NaH_2PO_4, 10 mM Tris/HCl, pH 8) and spotted on a nitrocellulose membrane (Protran NC transfer membrane, Schleicher & Schuell) with the help of a dot blot device (Schleicher & Schuell). The loaded nitrocellulose membrane was blocked in 5% fat-free dry milk in PBS/Tween (0.058 M $NaHPO_4$, 0.017 M NaH_2PO_4, 0.068 M NaCl, 0.5% Tween). The dots were incubated with an anti-NtAQP1 or an anti-NtPIP2.1 antibody raised in chicken or rabbit, respectively. The secondary antibody was linked to an alkaline phosphatase, which catalyzes a chemiluminescence reaction (CDP-Star, Applied Biosystems). Images were obtained with a ChemiDoc XRS (Bio-Rad). Signal intensity was evaluated by using Quantity One® software (Bio-Rad). The data presented were residing on four independent experiments.

Aquaporin Tetramer Separation—Aquaporin tetramer separation under nonreducing SDS-PAGE conditions was done in 9% SDS-polyacrylamide gels according to Laemmli (35). The samples were not heat-denatured, and the final concentrations in the sample buffer were 0.56 M Na_2CO_3, 12% sucrose, 0.3% SDS, 0.04% bromphenol blue. Proteins were transferred by electroblot (0.8 V/cm) onto PVDF membranes (Immobilon P, Millipore) in 10 mM CAPS, NaOH, pH 11.0, 10% methanol for 2 h. The membrane with the transferred proteins was subjected to aquaporin detection with specific antibodies as described above.

RESULTS

NtAQP1 or NtPIP2;1 were expressed in yeast and the cells were subjected to functional analysis for water transport or increased intracellular acidification under an inward-directed CO_2 gradient in a stopped flow spectrophotometer. In the case of CO_2 transport analysis, yeast cells were expressing a tobacco carbonic anhydrase in addition to the aquaporin. Intracellular acidification was observed via fluorescein fluorescence quenching, whereas yeast spheroplasts swelling due to water uptake was monitored by light scattering. It became evident that NtAQP1 was not functional with regard to water transport facilitation (Fig. 1*A*). In *Xenopus* oocytes, this and other PIP1 aquaporins displayed a very low or undetectable increase in

[2] The abbreviations used are: DDM, dodecylmaltoside; CAPS, *N*-cyclohexyl-3-aminopropanesulfonic acid; BiFC, bimolecular fluorescence complementation.

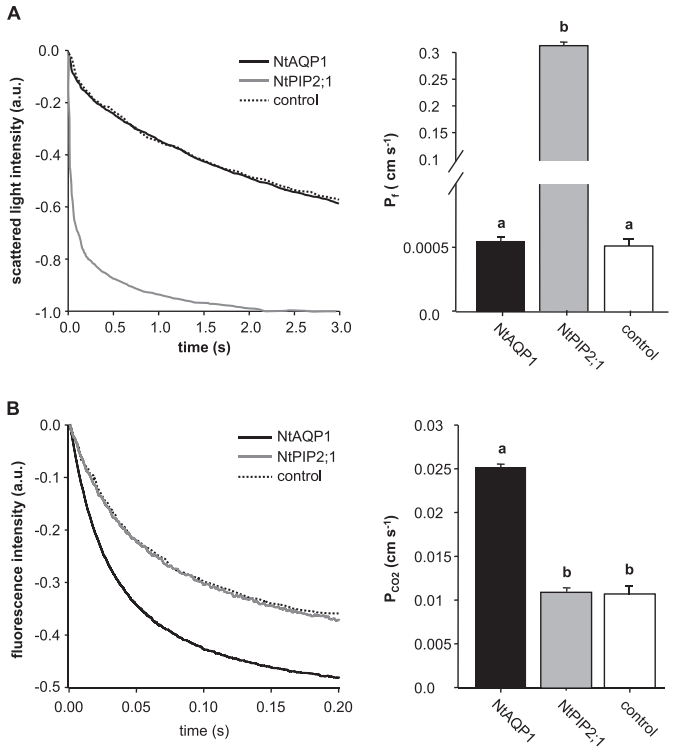

FIGURE 1. **Effect of NtAQP1 or NtPIP2;1 expression on CO_2-triggered intracellular acidification or water permeability of yeast plasma membranes.** *A*, water permeability. *Left panel*, representative time course of scattered light intensity in response to hypo-osmotic conditions. Yeast cells expressed NtAQP1, NtPIP2;1, or a control membrane protein (control) as indicated. *Right panel*, water permeability coefficient P_f (means ± S.E., $n \geq 100$). *p* values for allocation to different significance groups indicated by *different letters* were <0.005 as determined by a two-tailed Student's *t* test. *B*, CO_2-triggered intracellular acidification of yeast. *Left panel*, time course of intracellular acidification in response to CO_2. Yeast cells expressed NtAQP1, NtPIP2;1, or a control membrane protein (control) in addition to tobacco carbonic anhydrase as indicated. *Right panel*, CO_2 permeability coefficient P_{CO2} (means ± S.E., $n \geq 200$). *p* values for allocation to different significance groups indicated by *different letters* were <0.005 as determined by a two-tailed Student's *t* test. *a.u.*, arbitrary units.

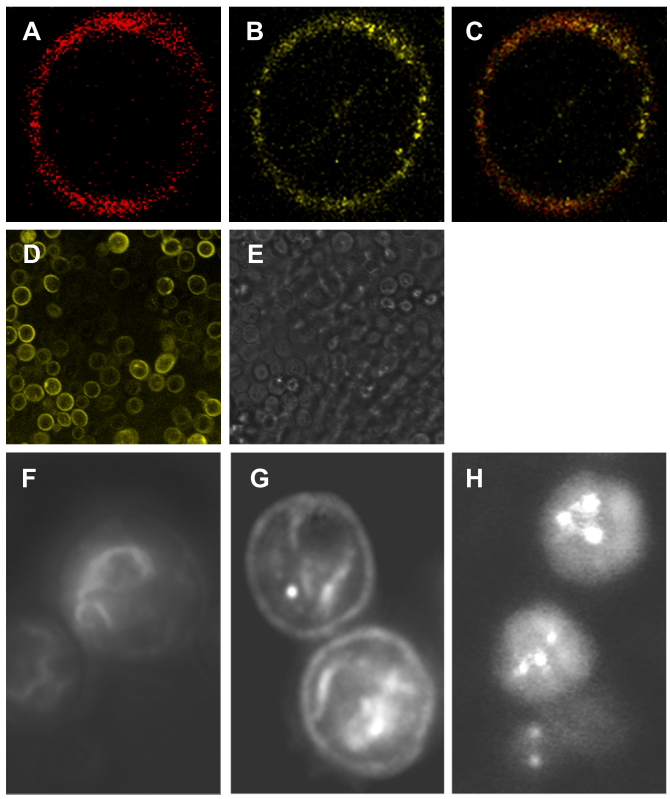

FIGURE 2. **Bimolecular fluorescence complementation in yeast expressing NtAQP1-YC and/or NtPIP2;1-YN.** *A*, yeast cell immediately after staining with FM4-64 imaged by confocal laser scanning at 670–750 nm. *B*, identical cell imaged by confocal laser scanning at 500–550 nm for BiFC-YFP visualization. *C*, merged image. *D*, wide field image at 500–550 nm of yeast cells expressing NtAQP1-YC and NtPIP2;1-YN. *E*, bright field image of cells depicted in *D*. *F*, wide field image of yeast cells expressing NtAQP1-YC and NtAQP1-YN at 500–550 nm. *G*, equivalent to *F* but with cells expressing NtAQP1YC and NtPIP2;1-YN. *H*, equivalent to *F* but with cells expressing NtPIP2;1-YC and NtPIP2;1-YN. *a.u.*, arbitrary units.

membrane water permeability. Thus, the results from the yeast system approximate what was obtained by analysis of oocytes expressing NtAQP1.

On the other hand, NtAQP1 had a comparatively high capacity to increase intracellular acidification rates in a CO_2 gradient (Fig. 1*B*). In contrast, NtPIP2;1 was not functional with this respect but very active as a true aquaporin (Fig. 1). In this regard, the two proteins exhibit inverted activity.

For the first assessment of the NtAQP1-NtPIP2;1 interaction, the proteins were subjected to a split YFP or bimolecular fluorescence complementation (BiFC) analysis. NtAQP1 or NtPIP2;1 were tagged with the C- or N-terminal half of YFP (YC or YN), respectively. Microscopic inspection of yeast cells expressing NtAQP1-YC and NtAQP1-YN or the respective constructs with NtPIP2;1 revealed a fluorescence spectrum that was superimposing that of YFP (data not shown). It was concluded that the detected emission was YFP-specific fluorescence. In certain areas, the YFP fluorescence in cells expressing the aquaporin-YC and aquaporin-YN constructs matches that of the plasma membrane-staining dye FM4-64 (Fig. 2, *A–C*). Because a YFP fluorescence signal was detected in these aquaporin YFP construct-expressing yeasts, it is possible that NtAQP1 and NtPIP2;1 form homotetramers. Coexpression of NtAQP1-YFP and NtPIP2;1-YFP constructs also revealed fluorescence, disregarding whether NtAQP1 or NtPIP2;1 carries the YC or YN tag, respectively. Accordingly, heterotetramer formation could be possible and is not a rare event as indicated by wide field images (Fig. 2*D*). Application of a colocalization matrix (YFP *versus* FM4-64) enabled us to estimate the relative abundance of NtAQP1 and NtPIP2;1 as well as that of the coexpressed aquaporins in the yeast plasma membrane (Fig. 2, *F–H*). For NtAQP1-YC coexpressed with NtAQP1-YN, 4.1% ($n = 39$) of total fluorescence was detected in the plasma membrane; the NtAQP1-YC and NtPIP2;1-YN combination revealed 14.2% ($n = 35$) and that of NtPIP2;1-YC and NtPIP2;1-YN 2.1% ($n = 37$) relative fluorescence in plasma membrane areas. If cells co-expressing NtPIP2;1-YC and NtPIP2;1-YN were subjected to a functional test, in comparison with nonfused aquaporins, reduced but significant activity for water transport was observed (Figs. 1*A* and 3*A*). Although the respective specificity of the aquaporins maintained when either NtAQP1 or NtPIP2;1 were expressed as BiFC constructs, the membrane diffusion rates were modified when NtAQP1-YC and NtPIP2;1-YN were both expressed in yeast cells. The water permeability was reduced but still substantial (Fig. 3*A*), whereas the CO_2-dependent cellular acidification was reduced to control values (Fig.

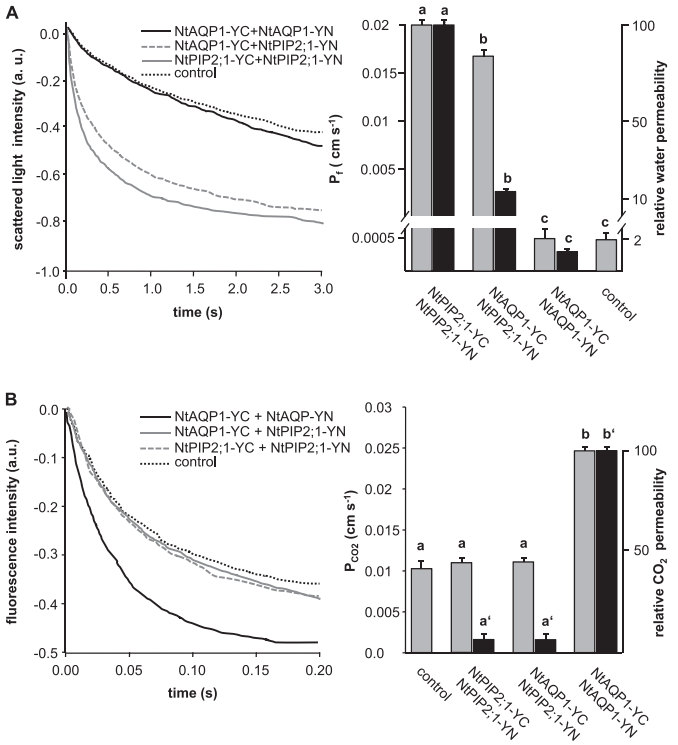

FIGURE 3. **Effect of BiFC-YFP aquaporin fusion proteins on CO_2-induced intracellular acidification and water permeability of yeast plasma membranes.** *A*, *left panel*, water uptake kinetics of yeasts expressing different BiFC-aquaporin fusion proteins as indicated. *Right panel*, calculated water permeability from raw data (*gray columns*) and water conductivity relative to the protein membrane fluorescence (*black columns*). The *control bar* depicts calculated water permeability. Relative water conductivity was not given as controls do not show aquaporin-related YFP fluorescence. Means ± S.E., $n = 1500$ (NtAQP1-YC+NtAQP1-YN), 1500 (NtAQP1-YC+NtPIP2;1-YN), 1300 (NtPIP2;1-YC+NtPIP2;1-YN), and 1000 (control). *p* values for allocation to different significance groups indicated by different letters were <0.005 as determined by a two-tailed Student's *t* test *B*, CO_2-induced intracellular acidification of yeast cells expressing aquaporin constructs as indicated. *Left panel*, CO_2-induced intracellular acidification rates. Calculated P_{CO2} data (*gray columns*) and values relative to the protein membrane fluorescence (*black columns*) are shown. The *control bar* depicts calculated water permeability. Relative CO_2 conductivity was not given as controls do not show aquaporin-related YFP fluorescence. Means ± S.E.; $n = 900$ (NtAQP1-YC+NtAQP1-YN), 800 (NtAQP1-YC+NtPIP2;1-YN), 800 (NtPIP2;1-YC+NtPIP2;1-YN), and 800 (control). *p* values for allocation to different significance groups indicated by *different letters* were <0.005 as determined by a two-tailed Student's *t* test. *a.u.*, arbitrary units.

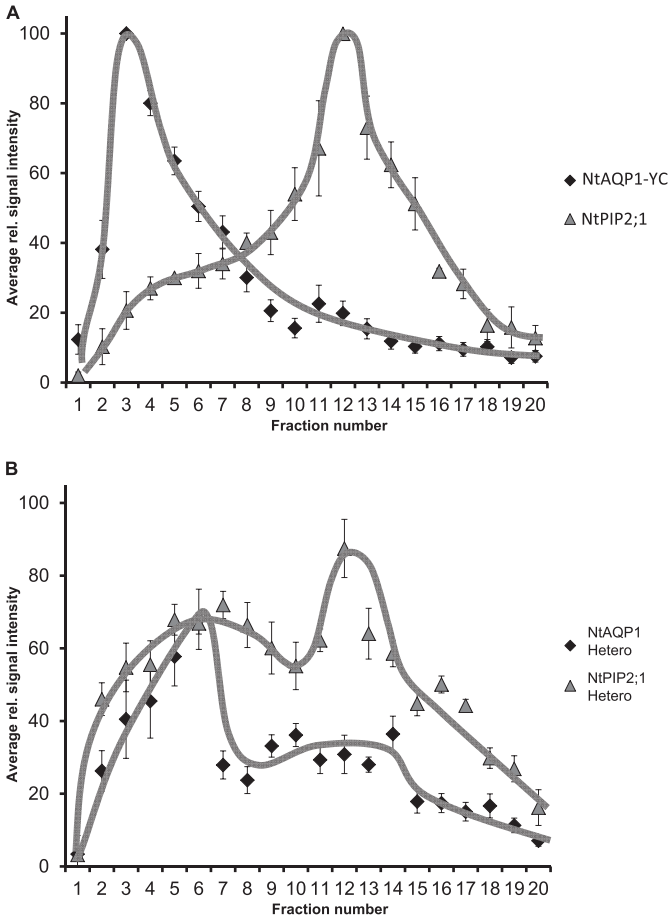

FIGURE 4. **Separation of aquaporin tetramers by column size exclusion chromatography.** *A*, size-fractionated plasma membrane proteins with a molecular mass larger than 80 kDa from yeast strains expressing NtAQP1 fused to a YFP C-terminal region (*Nt-YC*, *diamonds*) or NtPIP2.1 (*PIP2.1*, *triangles*). *B*, shown as described in *A*, but yeast strains expressing NtAQP1 were fused to a YFP C-terminal region, and NtPIP2.1 was probed with a NtAQP1 (*Nt Hetero*, *diamonds*) or a NtPIP2;1-specific antibody (*PIP2;1 Hetero*, *triangles*). For illustration of protein distribution a free hand trend line was added (NtAQP1, *black*; NtPIP2;1, *gray*). Data refer to relative signal distribution (means ± S.E.). *rel.*, relative.

3*B*). In the case of NtAQP1-YC and NtPIP2;1-YN coexpression, the obtained data and values related to the fluorescence in the plasma membrane were the sum of heterotetramers and homotetramers. Because the latter consisted of only one-half of the YFP, these complexes do not emit fluorescence and could thereby add an unaccounted factor to the activity calculation. Nevertheless, it appeared that coexpression of the aquaporins interferes with function.

At this point, it was indistinguishable whether the restored YFP fluorescence was caused by homotetramer interaction or formation of heterotetramers. In principle, aquaporin tetramers can be separated from monomers or dimers by size exclusion chromatography. However, because the size of NtAQP1 and NtPIP2;1 homo- and heterotetramers is very similar, it is impossible to divide and distinguish homo- or heterotetramer complexes by this technique directly. Therefore, solubilized plasma membrane proteins from yeast expressing the modified NtAQP1-YC, with a C-terminal extension of ~10 kDa, were compared with those expressing an unmodified NtPIP2;1. In this approach, the tetrameric proteins were well separated on a size exclusion chromatography column (Fig. 4*A*) as indicated by their relative elution maxima in fractions 3 (NtAQP1-YC) and 13 (NtPIP2;1). When coexpressed, the distinct peaks of NtAQP1-YC- or NtPIP2;1-eluted tetramers were reduced, and the tetramers also appeared in substantial in smaller or larger fractions, respectively amounts (Fig. 4*B*). This denotes for an interaction of the proteins, most likely as heterotetramers. It should be noted here, that due to the nonlinear shape of aquaporins, a careful size determination of the protein complexes with standard molecular weight markers appeared technically impossible and was therefore omitted. The findings from column chromatography were supported by the results of gel electrophoresis with yeast membrane proteins under nonreducing SDS-PAGE conditions and detection of aquaporins by specific antibodies (Fig. 5). Upon coexpression of NtAQP1 and NtPIP2;1, the electrophoretic separation pattern changed, and additional bands appeared, indicating for an interaction of different aqua-

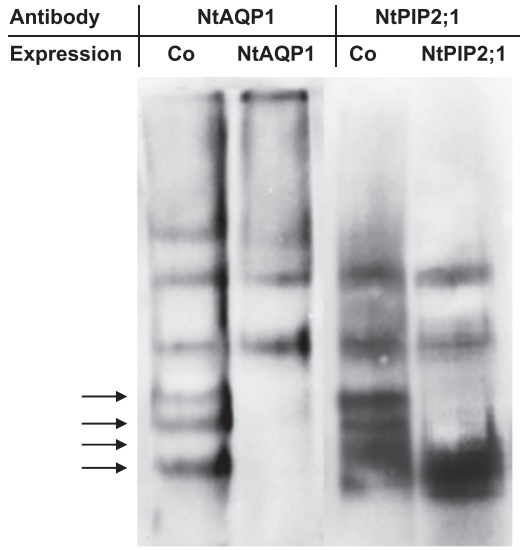

FIGURE 5. **Gel electrophoresis of yeast membrane proteins under nonreducing SDS-PAGE conditions and detection of aquaporins by specific antibodies.** Membrane proteins from yeast expressing either NtAQP1-YC or NtPIP2;1 or coexpressing both genes (*Co*) were separated in a polyacrylamide gel and detected with a NtAQP1-specific antibody (NtAQP1) or NtPIP2;1 specific antibody (NtPIP2;1). *Arrows* indicate the location of additional bands in samples from yeasts coexpressing NtAQP1-YC and NtPIP2;1. The depicted bands have an estimated molecular mass of at least 120 kDa. Membrane proteins from yeast cells not expressing NtAQP1-YC or NtPIP2;1 (not transformed or no induction of expression) do not lead to a signal with the employed NtAQP1- or NtPIP2;1-specific antibodies.

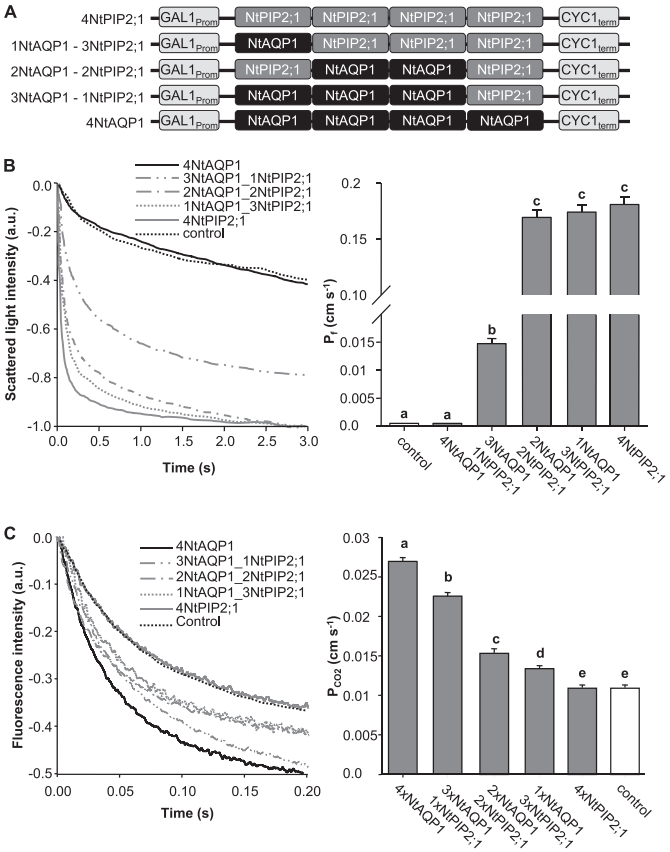

FIGURE 6. **Analysis of artificial tetramer NtAQP1 and NtPIP2;1 combinations.** *A*, schematic illustrating the employed artificial heterotetramer constructs. *B*, water permeability of yeast plasma membranes. *Left panel*, time course of scattered light intensity in response to yeast protoplast swelling. Yeast cells are expressing artificial heterotetramers as depicted in *A*. *Right panel*, corresponding water permeability coefficients (means ± S.E., $n \geq 30$). *p* values for allocation to different significance groups indicated by different letters were <0.005 as determined by two-tailed Student's *t* tests. *C*, intracellular acidification in response to CO_2. *Left panel*, time course of intracellular acidification of yeast cells expressing artificial tetramer combinations as depicted in *A*. *Right panel*, corresponding CO_2 permeability coefficients (means ± S.E. $n \geq 120$). *p* values for allocation to different significance groups indicated by different letters were <0.005 as determined by two-tailed Student's *t* tests. *a.u.*, arbitrary units.

porin isoforms. Again, precise determination of molecular masses by comparison to molecular markers was rendered difficult, as under these conditions, protein separation does not depend strictly on molecular weight but also depends on protein charge and shape (36).

Results from the three series of experiments (split YFP, functional assay, and the changed size distribution of the aquaporin constructs when coexpressed) argued for a heterotetramer formation. In addition, it is possible that the heterotetramer assemblage changes the specificity of aquaporin facilitated transport as indicated by the functional assays. To test this hypothesis, aquaporin tetramers with a definite aquaporin composition were expressed in yeasts, and the cells were examined for water- or CO_2-triggered intracellular acidification. The defined tetramers were encoded by gene constructs with four fused aquaporin sequences. The genes were constructed in a manner that NtAQP1 and NtPIP2;1 appeared in the tetramer in increasing and decreasing amounts, respectively (Fig. 6*A*). The expression levels of the five constructs under investigation was comparable as determined by Western blot analysis of proteins from yeast membranes with NtAQP1- or NtPIP2;1-specific antibodies (data not shown). Their functional analysis revealed that a facilitated water transport could not be observed when the tetramer consists of NtAQP1 only. In a 3NtAQP1 and 1NtPIP2;1 tetramer, a 30× increased water transport rate was observed. Maximum values were achieved by the 2NtAQP1 and 2NtPIP2;1, 1NtAQP1 and 3NtPIP2;1, and 4NtPIP2;1 constructs (Fig. 6*B*). In the case of CO_2-triggered intracellular acidification, only the 4NtAQP1 construct induced maximum values. These were significantly reduced if the tetramer contained 1NtPIP2;1 and 3NtAQP1 (Fig. 6*C*). The higher the amount of NtPIP2;1 in the construct, the lower the intracellular CO_2 acidification rate. The presence of a single NtAQP1 as cooporin was not sufficient to induce rates that were multiples of controls as it was observed for water transport and NtPIP2;1. It seems that high CO_2-driven intracellular acidification requires the presence of at least 3- or even 4NtAQP1 in a tetramer. In the intermediate configuration (2NtAQP1 and 2NtPIP2;1), P_f is fully increased, whereas P_{CO2} is just increased slightly.

DISCUSSION

We showed that the tobacco aquaporins under investigation displayed opposing functions with regard to water or CO_2 transport in the yeast system. NtPIP2;1 induced high water transport rates and gave no rise in CO_2-triggered intracellular acidification. NtAQP1 displayed no detectable function as a water transport facilitator but increased CO_2-triggered intracellular acidification rates.

In plants, NtAQP1 appeared to have a dual function. On one hand, it was found to increase photosynthesis rates, which are

limited by CO_2 availability in chloroplasts. Photosynthesis rates in accordance to NtAQP1 expression support the hypothesis of a CO_2 transport facilitator function in plants (22, 37). Dissimilar to leaves, in roots, a reduced hydraulic conductivity was observed in tobacco plants expressing an NtAQP1 antisense RNA, which suggests a role in water transport (38). Yet, the precise reason for this organ-specific functional divergence in tobacco is unknown. Pre-experiments showed that the NtAQP1 monomer was shifted in molecular weight in root cells. Whether this protein modification could be the reason for the NtAQP1-dependent increase in hydraulic conductivity or the modification is just coincidence, remains to be elucidated. According to reports on coexpression of maize aquaporins in oocytes (39) or maize leaf protoplasts (26, 41), it can be concluded that a missing function of PIP1 aquaporins as a water facilitator might, in general, reside on comparably lower or absent plasma membrane integration. Only when coexpressed with a PIP2, an effect on membrane integration leading to enhanced water transport rates was induced. If this effect occurs in tobacco roots, NtAQP1 function in root hydraulic conductivity also would be reasonable. However, in yeast, we could show that the tobacco aquaporin NtAQP1 was inserted into plasma membranes to a level twice as high as that of NtPIP2;1. This denotes that the comparably low water permeability of yeasts expressing NtAQP1 was not due to the deficiency of the aquaporin in plasma membranes. However, we could also observe a beneficial effect on membrane incorporation of PIP1/PIP2 coexpression. For some maize PIP2 members, regulation of aquaporin plasma membrane incorporation has been shown to be dependent on a diacidic ER export motif in the N terminus of the protein (41). In the case of NtAQP1 and NtPIP2;1, this structural detail is missing and accordingly is irrelevant to membrane targeting.

Similar to the observations made in oocytes (9), yeasts expressing NtAQP1 showed increased CO_2-triggered intracellular acidification rates. This confirms the comparability of the yeast system to the analysis of aquaporin effects in oocyte expression systems. Coexpression of NtAQP1 with NtPIP2;1 seems to allow formation of heterotetramers as indicated by the results from split YFP experiments, size exclusion chromatography, and gel electrophoresis. Aquaporins fused with N- or C-terminal parts of YFP in heterotetramers were shown to be reduced in the water transport capacity, although membrane incorporation rates were increased. In contrast, the CO_2-triggered intracellular acidification rates of yeasts expressing both aquaporins were reduced to control levels. As our data were obtained on aquaporin fusion proteins, nonfused PIP1 and PIP2 proteins could have higher or lower membrane incorporation rates when expressed in yeast and other heterologous or homologous systems. This observation should be studied when PIP1 or PIP2 function is investigated. Functional analysis of artificial tetramers with a defined proportion of NtAQP1 and NtPIP2;1 was employed to study the effect of tetramer composition on aquaporin function and indicated that aquaporin-dependent membrane permeability was modified by it. Strikingly, an aquaporin tetramer with a single NtPIP2;1 aquaporin already showed considerably high water transport rates. Two NtPIP2;1 proteins led to nearly maximal levels. This is in accordance to the finding that an aquaporin monomer is the functional unit for water transport (4, 42, 43). CO_2-triggered acidification rates, on the other hand, were at maximal levels only if the tetramer consists of only NtAQP1. One reason for this observation could be due to the differences in driving forces in comparison with those of water. Because the increasing number of NtAQP1 aquaporins in a tetramer lead to sequential increase in CO_2-triggered acidification, this function also could be related to something that is based on multimers. The cooperative effect on this function was reflected by a more sigmoid than linear increase of the acidification rates with increasing numbers of NtAQP1 in the tetramer. It resembles kinetics of allosteric enzymes (40, 44). The functional change could well reside on possible steric adjustments of an aquaporin monomer in the tetramer with consequences on function. However, in this case, NtAQP1 proteins also could generate a joint structure that ensures maximum CO_2 transport rates if the tetramer consists of only the PIP1 aquaporin. It is tempting to assume that the so-called fifth pore in the center of the tetramer is the respective structure (39).

Taken together, it became evident that PIP1 or PIP2 aquaporins have distinct functions. One rather indirectly leads to variation in aquaporin incorporation rates. The other directly relates to the facilitation of separate diffusion processes, for NtPIP2;1 that of water, for NtAQP1 that of CO_2-triggered intracellular acidification, which could be CO_2 diffusion. The aquaporins form heterotetramers, which modify the function as membrane transport facilitators of specific molecules.

Acknowledgments—We thank M. Engstler and N. Heddergott (University of Wuerzburg) for disposition of iMIC microscope. We also thank A. Starzinski-Powitz and A. Schreiner (University of Frankfurt) for plasmids pYC and pYN, as well as A. Bertl (Darmstadt University of Technology) for providing yeast strain W303 and C. Koch (University of Erlangen) for plasmid YEplac112. A plasmid containing the coding region of MDL1p was kindly provided by R. Tampé (University of Frankfurt). We are indebted to V. Endeward and G. Gros (Hannover Medical School) for carbonic anhydrase mass spectrometry analysis, and A. Terwisscha van Scheltinga as well as F. Rodrigues-Martinez (Max Planck Institute for Biophysics, Frankfurt, Germany) for substantial help in membrane protein solubilization experiments.

REFERENCES

1. Murata, K., Mitsuoka, K., Hirai, T., Walz, T., Agre, P., Heymann, J. B., Engel, A., and Fujiyoshi, Y. (2000) *Nature* **407,** 599–605
2. Sui, H., Han, B. G., Lee, J. K., Walian, P., and Jap, B. K. (2001) *Nature* **414,** 872–878
3. Strand, L., Moe, S. E., Solbu, T. T., Vaadal, M., and Holen, T. (2009) *Biochemistry* **48,** 5785–5793
4. Heymann, J. B., Agre, P., and Engel, A. (1998) *J. Struct. Biol.* **121,** 191–206
5. Preston, G. M., Carroll, T. P., Guggino, W. B., and Agre, P. (1992) *Science* **256,** 385–387
6. Nakhoul, N. L., Davis, B. A., Romero, M. F., and Boron, W. F. (1998) *Am. J. Physiol. Cell Physiol.* **274,** C543–548
7. Nakhoul, N. L., Hering-Smith, K. S., Abdulnour-Nakhoul, S. M., and Hamm, L. L. (2001) *Am. J. Physiol. Renal Physiol.* **281,** F255–263
8. Biela, A., Grote, K., Otto, B., Hoth, S., Hedrich, R., and Kaldenhoff, R. (1999) *Plant J.* **18,** 565–570
9. Uehlein, N., Lovisolo, C., Siefritz, F., and Kaldenhoff, R. (2003) *Nature* **425,** 734–737

10. Kaldenhoff, R., and Fischer, M. (2006) *Acta. Physiol.* (*Oxf.*) **187,** 169–176
11. Chaumont, F., Barrieu, F., Jung, R., and Chrispeels, M. J. (2000) *Plant Physiol.* **122,** 1025–1034
12. Chaumont, F., Barrieu, F., Wojcik, E., Chrispeels, M. J., and Jung, R. (2001) *Plant Physiol.* **125,** 1206–1215
13. Johanson, U., Karlsson, M., Johansson, I., Gustavsson, S., Sjövall, S., Fraysse, L., Weig, A. R., and Kjellbom, P. (2001) *Plant Physiol.* **126,** 1358–1369
14. Johansson, I., Karlsson, M., Johanson, U., Larsson, C., and Kjellbom, P. (2000) *Biochim. Biophys. Acta.* **1465,** 324–342
15. Kammerloher, W., Fischer, U., Piechottka, G. P., and Schäffner, A. R. (1994) *Plant J.* **6,** 187–199
16. Weig, A., Deswarte, C., and Chrispeels, M. J. (1997) *Plant Physiol.* **114,** 1347–1357
17. Marin-Olivier, M., Chevalier, T., Fobis-Loisy, I., Dumas, C., and Gaude, T. (2000) *Plant J.* **24,** 231–240
18. Moshelion, M., Becker, D., Biela, A., Uehlein, N., Hedrich, R., Otto, B., Levi, H., Moran, N., and Kaldenhoff, R. (2002) *Plant Cell* **14,** 727–739
19. Cooper, G. J., Zhou, Y., Bouyer, P., Grichtchenko, I. I., and Boron, W. F. (2002) *J. Physiol.* **542,** 17–29
20. Musa-Aziz, R., Chen, L. M., Pelletier, M. F., and Boron, W. F. (2009) *Proc. Natl. Acad. Sci. U.S.A.* **106,** 5406–5411
21. Uehlein, N., Otto, B., Hanson, D. T., Fischer, M., McDowell, N., and Kaldenhoff, R. (2008) *Plant Cell* **20,** 648–657
22. Flexas, J., Ribas-Carbó, M., Hanson, D. T., Bota, J., Otto, B., Cifre, J., McDowell, N., Medrano, H., and Kaldenhoff, R. (2006) *Plant J.* **48,** 427–439
23. Terashima, I., and Ono, K. (2002) *Plant Cell Physiol.* **43,** 70–78
24. Fetter, K., Van Wilder, V., Moshelion, M., and Chaumont, F. (2004) *Plant Cell* **16,** 215–228
25. Moshelion, M., Moran, N., and Chaumont, F. (2004) *Plant Physiol.* **135,** 2301–2317
26. Zelazny, E., Borst, J. W., Muylaert, M., Batoko, H., Hemminga, M. A., and Chaumont, F. (2007) *Proc. Natl. Acad. Sci. U.S.A.* **104,** 12359–12364
27. Endeward, V., Musa-Aziz, R., Cooper, G. J., Chen, L. M., Pelletier, M. F., Virkki, L. V., Supuran, C. T., King, L. S., Boron, W. F., and Gros, G. (2006) *FASEB J.* **20,** 1974–1981
28. Bertl, A., and Kaldenhoff, R. (2007) *FEBS Lett.* **581,** 5413–5417
29. van Heeswijk, M. P., and van Os, C. H. (1986) *J. Membr. Biol.* **92,** 183–193
30. Yang, B., Fukuda, N., van Hoek, A., Matthay, M. A., Ma, T., and Verkman, A. S. (2000) *J. Biol. Chem.* **275,** 2686–2692
31. Bracha-Drori, K., Shichrur, K., Katz, A., Oliva, M., Angelovici, R., Yalovsky, S., and Ohad, N. (2004) *Plant J.* **40,** 419–427
32. Kirber, M. T., Chen, K., and Keaney, J. F., Jr. (2007) *Nature Methods* **4,** 767–768
33. Shannon, C. E. (1948) *Bell Syst. Tech. J.* **27,** 379–423
34. Panaretou, B., and Piper, P. (2006) *Methods Mol. Biol.* **313,** 27–32
35. Laemmli, U. K. (1970) *Nature* **227,** 680–685
36. Hames, B. D., and Rickwood, D. (1981) in *Gel Electrophoresis of Proteins: A Practical Approach*, pp. 14–18, IRL Press, Ltd., Eynsham, England
37. Kaldenhoff, R. (2005) in *Progress in Botany* (Esser, K., Lüttge, U. E., Beyschlag, W., and Murata, J., eds) Vol. 67, pp. 206–215, Springer-Verlag Berlin Heidelberg, New York
38. Siefritz, F., Tyree, M. T., Lovisolo, C., Schubert, A., and Kaldenhoff, R. (2002) *Plant Cell* **14,** 869–876
39. Wang, Y., Cohen, J., Boron, W. F., Schulten, K., and Tajkhorshid, E. (2007) *J. Struct. Biol.* **157,** 534–544
40. Ricard, J., and Cornish-Bowden, A. (1987) *Eur. J. Biochem.* **166,** 255–272
41. Zelazny, E., Miecielica, U., Borst, J. W., Hemminga, M. A., and Chaumont, F. (2009) *Plant J.* **57,** 346–355
42. Cheng, A., van Hoek, A. N., Yeager, M., Verkman, A. S., and Mitra, A. K. (1997) *Nature* **387,** 627–630
43. Walz, T., Smith, B. L., Agre, P., and Engel, A. (1994) *EMBO J.* **13,** 2985–2993
44. Baudin, V., Pagnier, J., Kiger, L., Kister, J., Schaad, O., Bihoreau, M. T., Lacaze, N., Marden, M. C., Edelstein, S. J., and Poyart, C. (1993) *Protein Sci.* **2,** 1320–1330